

Feedback Control and Dynamic Behaviour of Z-Source Converter Fed Separately Excited DC Motor and Centrifugal Pump Set

Saswati Swapna Dash, Byamakesh Nayak, Subrat Kumar

Department of Electrical Engineering, YMCA University of Science & Technology,
Faridabad, Haryana, India

reachtoswapna@gmail.com

School of Electrical Engineering, KIIT University,
Bhubaneswar, Odisha, India

electricbkn11@gmail.com

Department of MMBPL, Bharat Petroleum Corporation Limited,
Mathura, Uttar Pradesh, India

subrat9257@gmail.com

Abstract—This paper presents an overall study of Feedback Control of Z-Source Converter Fed Separately excited DC motor with centrifugal Pump Set. Z-source converter can be used for both voltage buck and boost mode using LC impedance network. In this paper the dynamic modeling of Z-source with motor load and centrifugal pump set is carried out with new findings. The compensators for speed feedback loop are designed by taking average state space analysis and small signal model of the system. The feedback loop is designed by classical control methods. The experiment is done in MATLAB work environment and the result is verified by Simulation.

Keyword- Z-source chopper, Separately excited DC motor, Centrifugal pump, Small signal model, RHP zero.

I. INTRODUCTION

The application of power electronics increases with the increase of power utility. The LC-impedance network abbreviated as Z-source converter is used in almost in all modern power converters from ac-ac, ac-dc, dc-dc and dc-ac. the voltage buck and boost capability and polarity reversal are achieved by introducing shoot-through across the load in a Z-source converter [1]. The both voltage buck and boost capability of boost-buck converter and Z- source converter can be used in speed control of dc motor drive system [2]-[5]. In Z-source inverters the shoot through mode is hard to introduce because of chances of damaging the switches [6]. Buck and boost capabilities are achieved by two controlled electronics switches with inductors and capacitors arranged in X shape and a load of DC motor with a centrifugal pump set ,it is shown in Fig. 1.

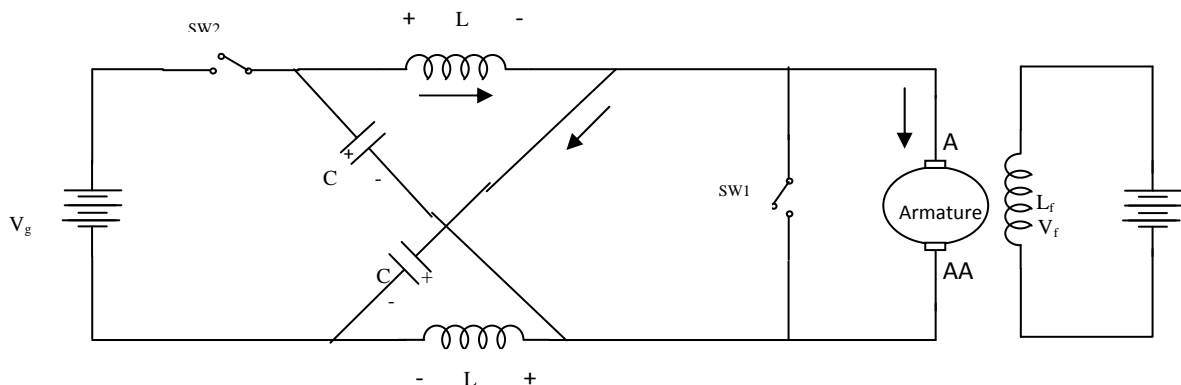


Fig.1. Circuit diagram of Z-source chopper controlled separately excited dc motor drive

In this paper, battery as input the Z-source chopper can be used in three modes such as: Boost mode with positive polarity, Boost mode with reverse polarity and Buck mode with reverse polarity in a definite duty cycle range. So by controlling the speed of a dc separately excited motor with centrifugal pump set in a wide range. Transient modeling and analysis is done for Z-source converter for constant load and the non minimum-phase response caused by battery side. The battery side phenomenon is associated with the value of inductance and capacitance in X shaped network and is studied using small-signal analysis to show the presence of the right-half-plane (RHP) zero in the control-to-command signals [7], [8], [9]. The maximum power point tracking for a solar pump system in a practical environment is performed with buck converter [10]. here the dynamic analysis is not investigated for controlling the flow of power. Again the dynamic performance is improved using the nonlinear control strategy based on feedback linearization [11].

II. STATE-SPACE AVERAGE ANALYSIS OF Z-SOURCE CHOPPER WITH MOTOR LOAD

Operation of Z-source chopper with motor load can be explained in two modes. Assuming continuous conduction mode, there are two modes one is called shoot-through mode, where load is shorted by turning on the switch-1 and other is input connected mode where switch-2 is on to connect the input to load. As shown in Fig. 1, the converter with the motor and centrifugal pump has five storing devices so five state variables are needed to represent the state-space average model [12], [13], [14]. The simple separately excited DC motor is used in this investigation. The load torque here is the mechanical torque (T_l) of the pump, which is directly proportional to the ‘head’ of the pump and here it is considered as a non-linear function of the motor speed i.e. $K_1\omega_m^2$. where $K_1 = 9.6 \times 10^{-5}$. The KVL, KCL expression in terms of the inductor current, armature current and capacitor voltage when switch-1 is on (switch-2 is off) are given by,

$$L \frac{di_l}{dt} = v_c \tag{1}$$

$$L_a \frac{di_1}{dt} + R_a i_1 + K_b \omega_m = 0 \tag{2}$$

$$C \frac{dv_c}{dt} = -i_l \tag{3}$$

Where $L, i_l, V_{in}, L_a, i_1, R_a, K_b, \omega_m, v_c, C$ are inductance in henry, inductor current in ampere, input voltage in volt, armature inductance in henry, armature current in ampere, armature resistance in ohm, back emf constant in N-m/amp, angular speed in rad/sec, capacitor voltage in volt and capacitance in mF respectively. Now the fundamental torque equation for the motor-load system is given by (4),

$$T_e - T_l = j \frac{d\omega_m}{dt} + B\omega_m \tag{4}$$

The above equation can be written as follows:

Since,
$$\left. \begin{aligned} T_e &= K_b i_1 \\ T_l &= K_1 \omega_m^2 \quad (\text{For centrifugal pump}) \end{aligned} \right\} \tag{5}$$

Now putting all the values in (4), and differentiating both sides,

$$j\dot{a} + Ba + 2K_1\omega_m a = K_b \frac{di_1}{dt} \tag{6}$$

Where
$$\frac{d\omega_m}{dt} = a \tag{7}$$

Where j, T_e, T_l, B, a represent moment of inertia of motor in $kg\cdot m^2$, instantaneous torque in N-m, load torque in N-m, viscous friction in N-m-s/rad and rate of change of speed respectively. The (1), (2), (3), (5) and (7) can be represented in state-space form as follows:

$$\begin{bmatrix} \frac{di_l}{dt} \\ \frac{di_1}{dt} \\ \frac{dv_c}{dt} \\ \frac{d\omega_m}{dt} \\ \frac{da}{dt} \end{bmatrix} = \begin{bmatrix} 0 & 0 & \frac{1}{L} & 0 & 0 \\ 0 & -\frac{R_a}{L_a} & 0 & -\frac{K_b}{L_a} & 0 \\ -\frac{1}{C} & 0 & 0 & 0 & 0 \\ 0 & 0 & 0 & 0 & 1 \\ 0 & \frac{-K_b R_a}{L_a j} & 0 & \frac{-K_b^2}{L_a j} & \frac{-(B+2K_1\omega_m)}{j} \end{bmatrix} \begin{bmatrix} i_l \\ i_1 \\ v_c \\ \omega_m \\ a \end{bmatrix} + \begin{bmatrix} 0 \\ 0 \\ 0 \\ 0 \\ 0 \end{bmatrix} \tag{8}$$

$$A_1 = \begin{bmatrix} 0 & 0 & \frac{1}{L} & 0 & 0 \\ 0 & -\frac{R_a}{L_a} & 0 & -\frac{K_b}{L_a} & 0 \\ -\frac{1}{C} & 0 & 0 & 0 & 0 \\ 0 & 0 & 0 & 0 & 1 \\ 0 & \frac{-K_b R_a}{L_a j} & 0 & \frac{-K_b^2}{L_a j} & \frac{-(B+2K_1\omega_m)}{j} \end{bmatrix} \text{ and } B_1 U_1 = \begin{bmatrix} 0 \\ 0 \\ 0 \\ 0 \\ 0 \end{bmatrix} \tag{9}$$

Similarly when switch-1 is off and the switch-2 is on. Based on KCL and KVL, the equations can be written as:

$$L_a \frac{di_1}{dt} + R_a i_1 + L \frac{di_l}{dt} + K_b \omega_m - v_c = 0 \tag{10}$$

$$L \frac{di_l}{dt} = v_g - v_c \tag{11}$$

Substituting (11) in (10), the resulting equation is as follows:

$$L_a \frac{di_1}{dt} + R_a i_1 + v_g - v_c + K_b \omega_m = v_c \tag{12}$$

$$C \frac{dv_c}{dt} = v_g - v_c \tag{13}$$

$$j \frac{d\omega_m}{dt} = K_b i_1 - K_1 \omega_m^2 - B \omega_m \tag{14}$$

The state-space form of above equations can be represented as follows:

$$\begin{bmatrix} \frac{di_1}{dt} \\ \frac{di_l}{dt} \\ \frac{dv_c}{dt} \\ \frac{d\omega_m}{dt} \\ \frac{da}{dt} \end{bmatrix} = \begin{bmatrix} 0 & 0 & -\frac{1}{L} & 0 & 0 \\ 0 & -\frac{R_a}{L_a} & \frac{2}{L_a} & -\frac{K_b}{L_a} & 0 \\ \frac{1}{C} & -\frac{1}{C} & 0 & 0 & 0 \\ 0 & 0 & 0 & 0 & 1 \\ 0 & -\frac{K_b R_a}{L_{aj}} & \frac{2K_b}{L_{aj}} & -\frac{K_b^2}{L_{aj}} & \frac{-(B+2K_1\omega_m)}{j} \end{bmatrix} \begin{bmatrix} i_1 \\ i_l \\ v_c \\ \omega_m \\ a \end{bmatrix} + \begin{bmatrix} \frac{v_g}{L} \\ -\frac{v_g}{L_a} \\ 0 \\ 0 \\ -\frac{v_g K_b}{L_{aj}} \end{bmatrix} \tag{15}$$

Where $A_2 = \begin{bmatrix} 0 & 0 & -\frac{1}{L} & 0 & 0 \\ 0 & -\frac{R_a}{L_a} & \frac{2}{L_a} & -\frac{K_b}{L_a} & 0 \\ \frac{1}{C} & -\frac{1}{C} & 0 & 0 & 0 \\ 0 & 0 & 0 & 0 & 1 \\ 0 & -\frac{K_b R_a}{L_{aj}} & \frac{2K_b}{L_{aj}} & -\frac{K_b^2}{L_{aj}} & \frac{-(B+2K_1\omega_m)}{j} \end{bmatrix}$ and $B_2 U_2 = \begin{bmatrix} \frac{v_g}{L} \\ -\frac{v_g}{L_a} \\ 0 \\ 0 \\ -\frac{v_g K_b}{L_{aj}} \end{bmatrix}$

Let the switching function of self commutated controlled switch-1 and switch-2 is q_1 and q_2 respectively.

Assuming the continuous conduction mode, the averaged model is obtained by substituting d for q_1 and $1-d$ for q_2 . The state-space average model is represented as follows:

$$\dot{X} = AX + BU$$

$$Y = CX$$

Where $A = dA_1 + (1-d)A_2$ and

$$BU = dB_1 U_1 + (1-d)B_2 U_2 \tag{16}$$

Putting the values in (16),

$$A = \begin{bmatrix} 0 & 0 & \frac{(2d-1)}{L} & 0 & 0 \\ 0 & -\frac{R_a}{L_a} & \frac{2(1-d)}{L_a} & -\frac{K_b}{L_a} & 0 \\ -\frac{(2d-1)}{C} & -\frac{(1-d)}{C} & 0 & 0 & 0 \\ 0 & 0 & 0 & 0 & 1 \\ 0 & -\frac{K_b R_a}{L_{aj}} & \frac{2K_b(1-d)}{L_{aj}} & -\frac{K_b^2}{L_{aj}} & \frac{-(B+2K_1\omega_m)}{j} \end{bmatrix}, BU = \begin{bmatrix} \frac{v_g}{L}(1-d) \\ -\frac{v_g}{L_a}(1-d) \\ 0 \\ 0 \\ -\frac{v_g K_b}{L_{aj}}(1-d) \end{bmatrix} \tag{17}$$

Hence the state-space average form can be written as follows:

$$\begin{bmatrix} \frac{di_1}{dt} \\ \frac{di_l}{dt} \\ \frac{dv_c}{dt} \\ \frac{d\omega_m}{dt} \\ \frac{da}{dt} \end{bmatrix} = \begin{bmatrix} 0 & 0 & \frac{(2d-1)}{L} & 0 & 0 \\ 0 & -\frac{R_a}{L_a} & \frac{2(1-d)}{L_a} & -\frac{K_b}{L_a} & 0 \\ \frac{(2d-1)}{C} & -\frac{(1-d)}{C} & 0 & 0 & 0 \\ 0 & 0 & 0 & 0 & 1 \\ 0 & -\frac{K_b R_a}{L_{aj}} & \frac{2K_b(1-d)}{L_{aj}} & -\frac{K_b^2}{L_{aj}} & \frac{-(B+2K_1\omega_m)}{j} \end{bmatrix} \begin{bmatrix} i_1 \\ i_l \\ v_c \\ \omega_m \\ a \end{bmatrix} + \begin{bmatrix} \frac{v_g}{L}(1-d) \\ -\frac{v_g}{L_a}(1-d) \\ 0 \\ 0 \\ -\frac{v_g K_b}{L_{aj}}(1-d) \end{bmatrix} \tag{18}$$

III. MODELLING OF CENTRIFUGAL PUMP

The affinity law is used to draw the performance curve of head and flow rate at the nominal speed. The flow rate Q is directly proportional to impeller speed and the head (H) is directly proportional to square of speed ω_m . Since the hydraulic power (P) is directly proportional to the head and flow rate therefore it is proportional to the cube of speed (ω^3).i.e. $K_1 \omega_m^3$.this law is applicable only above the threshold speed (ω_s).For less than the

threshold value the pressure produced by the pump is less than the static pressure and the rotation just circulate water within the pump. The characteristic of centrifugal pump with valve completely opened is illustrated in Fig.2 and the speed Vs centrifugal load torque graph is shown in Fig. 3.

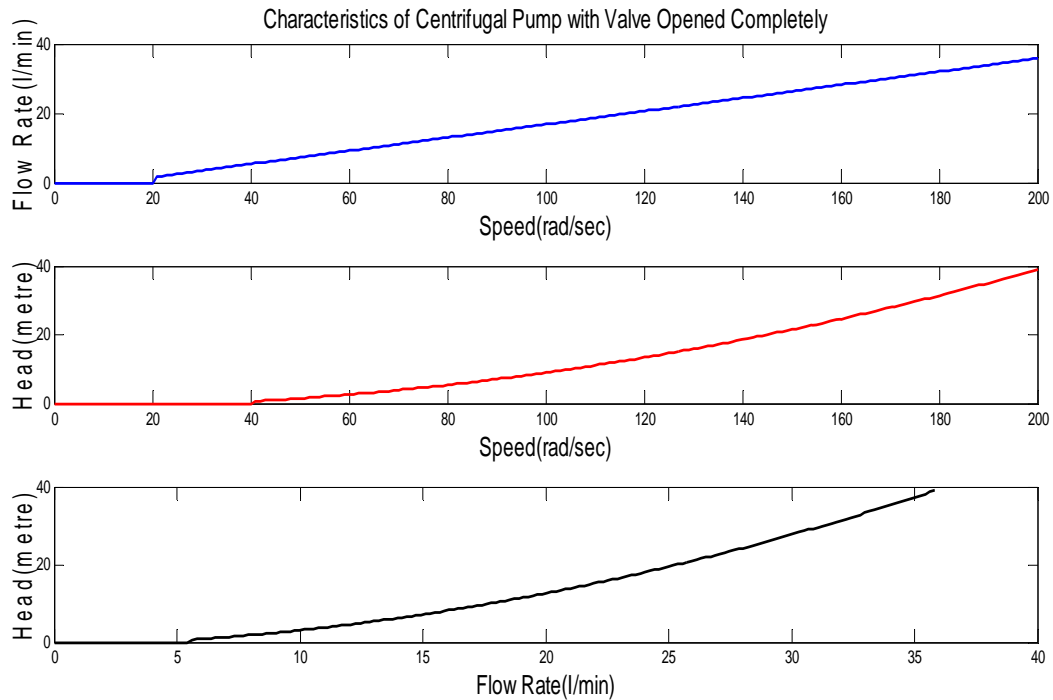


Fig.2. Characteristics of centrifugal pump with valve completely opened

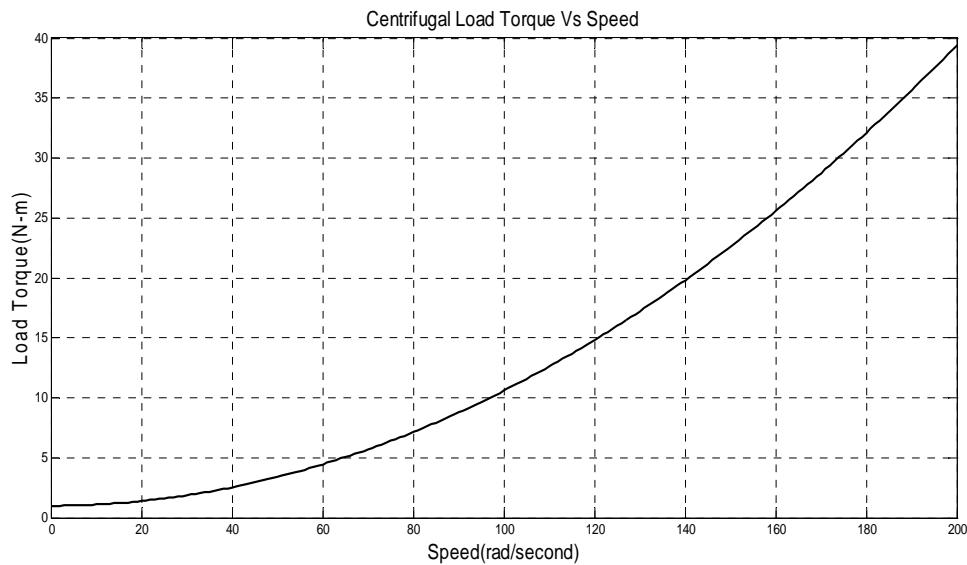


Fig. 3 Speed (ω_s) Vs Centrifugal Load Torque (T_l)

$$\left. \begin{aligned} Q &= a\omega - b \text{ (Where } \omega \geq \text{Threshold speed } (\omega_s)) \\ Q &= 0 \text{ (When } \omega \leq \text{Threshold speed } (\omega_s)) \end{aligned} \right\} \quad (19)$$

The value of ‘a’ and ‘b’ depend upon the static head and decreases with the increase of the pumping head and it has maximum value when the discharge valve is fully opened.[refieec paper]

The head equation can be written as

$$H = c\omega^2 - d\omega \quad (20)$$

Where the values of ‘c’ and ‘d’ depend on the valve setting. Since the hydraulic power is proportional to the head flow rate product. It is represented as:

$$P_h = c_1\omega^3 - c_2\omega^2 + c_3\omega \quad (21)$$

The Torque developed by the motor depends upon the head and therefore it is directly proportional to the square of the speed. To start the centrifugal pump, a breakaway torque of above 10-20% of nominal torque is required to overcome the static friction of the moving part involved. For variable head drive system, the speed of the motor is required to be controlled. In this paper, the speed is regulated depending on the head of the system. The Z-source chopper is used here to control the speed of the motor by controlling the armature voltage below and above the input battery voltage. For variable head drive systems, two methods can be adopted: (a) Changing speed of the motor keeping flow rate constant (b) Changing flow rate keeping speed constant. Here the first method is proposed in this paper.

IV. SMALL SIGNAL ANALYSIS

The state-space average model of Z-source converter with active machine load shown in (18) has non linear in nature as the control parameter (d) is in matrix A. Therefore small-signal analysis is required to make the state-space to be linear. Due to small variation of \hat{d} in steady state D the state variables are changed to $i_1 + \hat{i}_1, i_1 + \hat{i}_1, V_c + \hat{v}_c$ and $\omega_m + \hat{\omega}_m$. Assuming constant load torque and without disturbance in input voltage the state-space average model (18) with small perturbation is modified as follows:

$$\begin{bmatrix} \frac{d(i_1 + \hat{i}_1)}{dt} \\ \frac{d(i_1 + \hat{i}_1)}{dt} \\ \frac{d(V_c + \hat{v}_c)}{dt} \\ \frac{d(\omega_m + \hat{\omega}_m)}{dt} \\ \frac{d(a + \hat{a})}{dt} \end{bmatrix} = \begin{bmatrix} 0 & 0 & \frac{2(D + \hat{d}) - 1}{L} & 0 & 0 \\ 0 & -\frac{R_a}{L_a} & \frac{2(1 - D - \hat{d})}{L_a} & -\frac{K_b}{L_a} & 0 \\ -\frac{2(D + \hat{d}) - 1}{C} & -\frac{(1 - D - \hat{d})}{C} & 0 & 0 & 0 \\ 0 & 0 & 0 & 0 & 1 \\ 0 & -\frac{K_b R_a}{L_{aj}} & \frac{2K_b(1 - D - \hat{d})}{L_{aj}} & -\frac{K_b^2}{L_{aj}} & \frac{-(B + 2K_1 \omega_m)}{j} \end{bmatrix} \begin{bmatrix} i_1 + \hat{i}_1 \\ i_1 + \hat{i}_1 \\ V_c + \hat{v}_c \\ \omega_m + \hat{\omega}_m \\ a + \hat{a} \end{bmatrix} + \begin{bmatrix} \frac{V_g(1 - D - \hat{d})}{L} \\ -\frac{V_g(1 - D - \hat{d})}{L_a} \\ 0 \\ 0 \\ -\frac{V_g K_b(1 - D - \hat{d})}{L_{aj}} \end{bmatrix} \quad (22)$$

Subtracting steady-state representation of (18) from (22) and neglecting higher order perturbation terms the small-signal model of Z-source without any change in mechanical load torque can be written as follows:

$$\begin{bmatrix} \frac{d\hat{i}_1}{dt} \\ \frac{d\hat{i}_1}{dt} \\ \frac{d\hat{v}_c}{dt} \\ \frac{d\hat{\omega}_m}{dt} \\ \frac{d\hat{\omega}_m}{dt} \end{bmatrix} = \begin{bmatrix} 0 & 0 & -\frac{(1 - 2D)}{L} & 0 & 0 \\ 0 & -\frac{R_a}{L_a} & \frac{2(1 - D)}{L_a} & -\frac{K_b}{L_a} & 0 \\ \frac{(1 - 2D)}{C} & -\frac{(1 - D)}{C} & 0 & 0 & 0 \\ 0 & 0 & 0 & 0 & 1 \\ 0 & -\frac{K_b R_a}{L_{aj}} & \frac{2K_b(1 - D)}{L_{aj}} & -\frac{K_b^2}{L_{aj}} & \frac{-(B + 2K_1 \omega_m)}{j} \end{bmatrix} \begin{bmatrix} \hat{i}_1 \\ \hat{i}_1 \\ \hat{v}_c \\ \hat{\omega}_m \\ \hat{a} \end{bmatrix} + \begin{bmatrix} \frac{2V_c - V_g}{L} \\ \frac{V_g - 2V_c}{L_a} \\ \frac{(i_1 - 2i_1)}{C} \\ 0 \\ \frac{K_b(V_g - 2V_c)}{L_{aj}} \end{bmatrix} [\hat{d}] \quad (23)$$

The small signal step responses for inductor current, armature current, capacitor voltage, speed and rate of change of speed are represented in following fig.4

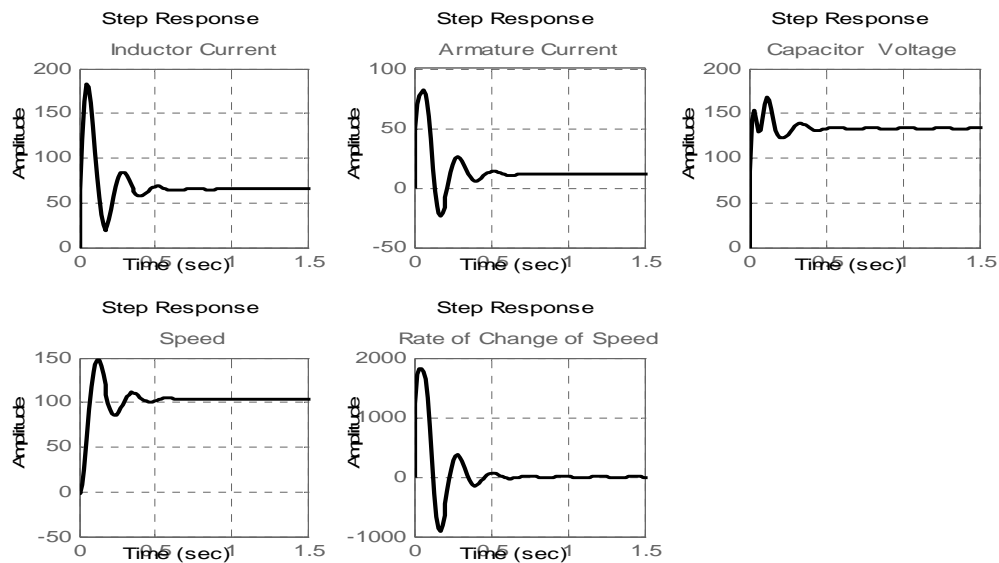


Fig.4. Small signal step responses for Inductor current, Armature current, Capacitor voltage, Speed and Rate of change of speed

V. STEADY-STATE ANALYSIS AND TRANSFER FUNCTION

The steady-state equations can be derived from average state-space model (18) and represented as follows:

$$V_c = \frac{(1-D)V_g}{(1-2D)} \tag{24}$$

$$i_1 = \frac{(1-D)i_1}{(1-2D)} \tag{25}$$

$$\frac{K_b\omega_m + R_a i_1}{V_g} = \frac{(1-D)}{(1-2D)} \tag{26}$$

$$T_L = K_b i_1 - B\omega_m \tag{27}$$

In previous papers where in Z-source converters consist of one switch and one diode. Due to such configuration when duty cycle is above 0.5 the diode will remain on because of the forward biased condition. Therefore only Boost operation is possible in such converters. Where in this paper two switches are used which overcomes the draw backs of previous configuration and can achieve the three modes for (boost in positive polarity, buck and boost in reverse polarity) by varying the duty ratio from 0 to 1. Fig. 5 shows the boost and boost-buck capability with polarity reversal of Z-source chopper. The Z-source chopper posses boost capability with same polarity as input in the duty ratio range between $0 < D < 0.5$ and both boost and buck capability with reverse polarity in the duty ratio range between $0.5 < D < 1$.

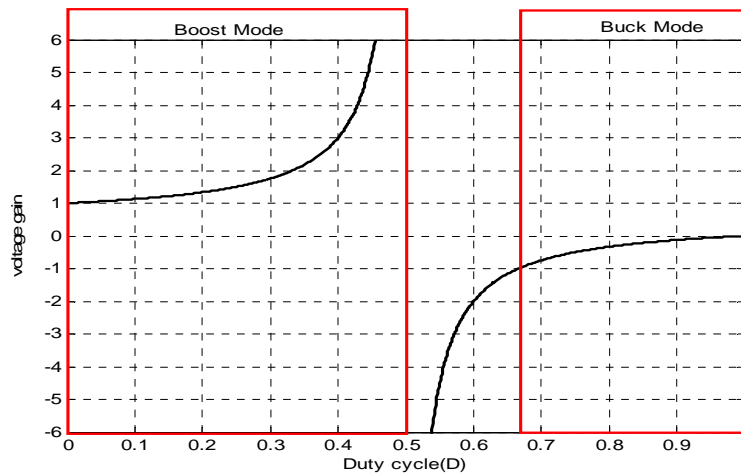


Fig. 5. Modulus of voltage gain versus duty cycle of Z-source converter controlled separately excited dc motor drive

The small signal model parameters are given in the Table-I,

TABLE II
Small Signal Model Parameters

V_g	R_a	L_1	L_2	C	D	B	J	f_s	K_b	K_1
48V	0.5Ω	8mH	10mH	1mF	0.3	0.02N- m-s/rad	0.05Kg- m ²	20kHz	1.23N- m/amp	9.6 × 10 ⁻⁴

VI. TRANSIENT ANALYSIS

It is important to study the transient behavior of Z-source chopper with machine load and centrifugal pump set, Before analyzing the closed loop control of separately excited dc motor, Many methods for modeling of power converters have been reported in the literature [8], [12], [15]. Here commonly adopted average state-space analysis with small-signal method is used to study the transient behavior of open loop system with step changes of duty cycle. as discussed previously in this phenomena three modes of operation occurs as the value of D varies from 0 to 1.so considering this three modes of operation are present The Z-source chopper posses boost capability with positive polarity as input in the duty ratio range between $0 < D < 0.5$, boost capability with reverse polarity in the duty ratio range between $0.5 < D < 0.67$ and buck capability in reverse polarity in the duty ratio range between $0.6 < D < 1$. For the wide speed range operation of dc motor, it is necessary to observe the movements of zeros and poles in order to maintain acceptable performance and stability [16], [17], [18].so describing movements of poles and zeros in all the duty ranges as follows.

A. ($0 < D < 0.5$) Boost Mode with Positive Polarity

In this duty ratio range as illustrated in the Fig.6, the dominant poles moves towards the imaginary axis and the non dominant poles moves away from the imaginary axis. So the settling time and overshoot increases. The magnitude of imaginary part of dominant poles reduces as $d > 0.5$ which reduces the oscillation.

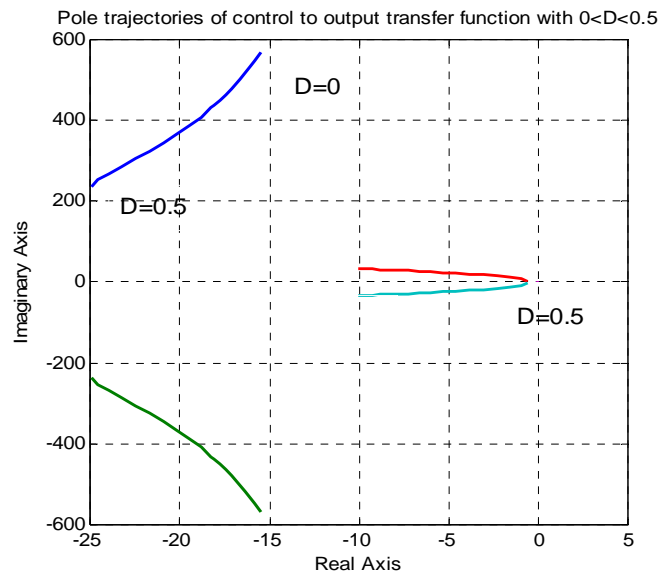


Fig. 6. Pole trajectories of control-to-output transfer function for change of D from 0 to 0.5

B. ($0.5 < D < 0.67$) Boost Capability in Reverse Polarity

In this duty ratio range the dominant poles moves away from the imaginary axis and the non dominant poles moves towards the imaginary axis as the D increases from 0.5 to 0.67. so the settling time, overshoot decreases in this range with increase of D. it is shown in fig.7.

Pole trajectories of control-to-output transfer function with change in D from 0.51 to 0.67

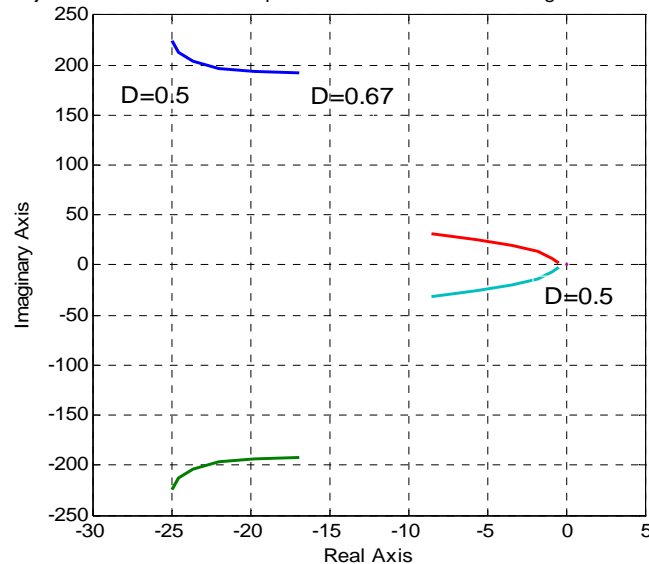


Fig. 7. Pole trajectories of control-to-output transfer function for change of D from 0.5 to 0.67

C. ($0.67 < D < 1$) Buck Capability in Reverse Polarity

In this case, the non dominant poles becomes dominant and dominant poles become non dominant compared to duty ratio range $0 < D < 0.5$ the real parts of dominant poles moves towards imaginary axis but the magnitude of imaginary part increases as D increases to 1. The non dominant poles also moves towards imaginary axis which increases the settling time and overshoot with large oscillations with D varies from 0.67 to 1. Hence here all the poles move towards imaginary axis so the noise rejection capability increases as in fig.8.

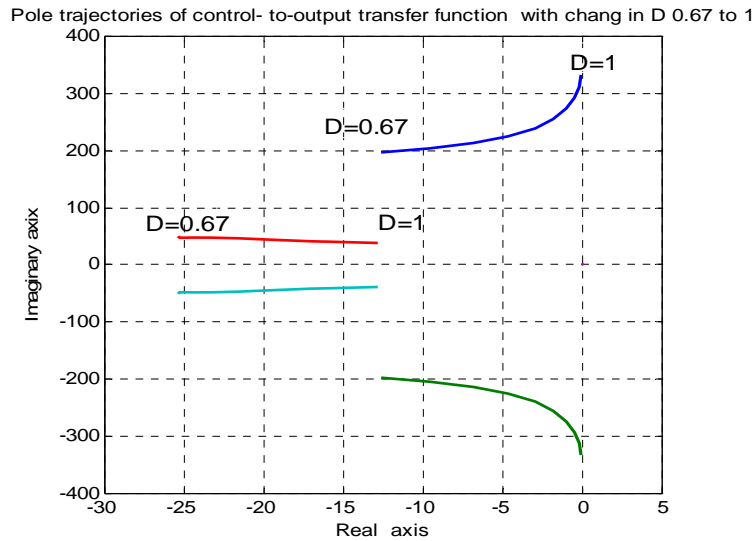


Fig. 8. Pole trajectories of control-to-output transfer function for change of D from 0.67 to 1

Where $G_{ild}(S)$, $G_{i1d}(S)$, $G_{vcd}(S)$, $G_{wd}(S)$, $G_{ad}(S)$ are called control-to-inductor current, control-to-armature current, control-to-capacitor voltage, control-to-speed and control to rate of change of speed transfer functions respectively. The right-half-plane zero of control-to-output transfer functions for different value of duty ratio with constant Z-source parameters ($L=8mH$ and $C=1mF$) are shown in Table III. Here the control-to-inductor current transfer function possesses the minimum-phase transient because of non presence of RHP zero in the boost mode with positive polarity but when the D varies from 0.5 to 1 there is presence of RHP zero whereas, the other transfer functions have non minimum-phase transient. With step change of D from 0.3 to 0.4 at 3seconds and 0.6 to 0.7 at 4 seconds the simulations are carried out and represented in Fig. 9(a, b, c, d) and Fig. 10(a, b, c, d) respectively. These figures show the step responses of control-to-inductor current, control-to-armature current, control-to-capacitor voltage and control-to-speed respectively. This is because of absence of RHP zero during D from 0 to 0.5 but when D value increase from 0.5 onwards there is dip due to RHP zero. Because of this the system stability may be affected. Therefore the inductor current is taken as feedback inner loop instead of armature current. Again the RHP zero is present in the capacitor voltage and the speed during the D varies from 0 to 0.5, the dip does not exist in the speed and capacitor voltage response because of RHP zero remain farthest from imaginary axis. Here there is no dip in inductor current during step change. The figure of control-to-armature current clearly shows the decrease of armature current at the instant of transient before rising towards its new steady-state value.

TABLE IV
RHP Zero for Change of D

D	$G_{ild}(S)$	$G_{i1d}(S)$	$G_{vcd}(S)$	$G_{wd}(S)$	$G_{ad}(S)$
0.0	No-RHP	140.38	576.7	140.38	140.38
0.2	No-RHP	106.20	385.52	106.20	106.20
0.4	No-RHP	50.00	184.42	50.00	50.00
0.6	$9.5 \pm j197.62, 3.29$	No-RHP	$8.86 \pm j82.74$	No-RHP	No-RHP
0.8	$24.21 \pm j68.69, 123.88$	No-RHP	No-RHP	No-RHP	No-RHP

To demonstrate the shifting of four complex conjugate poles with change in duty ratio (D) the poles trajectories are drawn in complex plane and it is shown in Fig. 5, which clearly shows the shifting of dominant poles towards the imaginary axis with increase of D from 0 to 0.5. The shifting of poles towards imaginary axis are observed which increases the system damping with a reduced overshoot and undershoot but an increased rise time and settling time. But when $D > 0.5$ and increasing, the shifting of dominant poles are away from the imaginary axis, which reduces the system damping and settling time as shown in Fig. 9(a, b, c, d) and Fig. 10(a, b, c, d). Table The Table V shows the movements of poles of control-to-output transfer function with constant D when L and C vary individually. For a more effective implementation of feedback control for boosting operation of Z-source chopper for speed control, it is recommended that instead of armature current feedback, the inductor current feedback can be used, which eliminates the non minimum-phase effect. In both the boost mode with positive polarity and reverse polarity, when 'L' and 'C' increases the dominant poles moves towards the imaginary axis. Hence the overshoot and settling time increases. In the buck mode with reverse polarity, the

similar phenomena occurs in case of change of 'L' but as the capacitor value changes from 1mf to 5mf, the dominant poles slightly moves away from imaginary axis resulting reduced settling time.

TABLE VIII
Movement of Poles for Individual Change of L and C

PARAMETERS	D	POLES POSITION
L=0.008H,C=0.001F	0.3	$-20.9 \pm j346, -5 \pm j23$
L=0.016H, C=0.001F		$-22.8 \pm j332, -3.5 \pm j16.5$
L=0.008H,C=0.005F		$-21.66 \pm j159.3, -4.7 \pm j21.6$
L=0.008H,C=0.001F	0.6	$-22.1 \pm j197.2, -4.22 \pm j19.58$
L=0.016H, C=0.001F		$-23.5 \pm j191.3, -2.8 \pm j14.3$
L=0.008H,C=0.005F		$-23.6 \pm j97.1, -2.8 \pm j17.5$
L=0.008H,C=0.001F	0.8	$-4.1 \pm j230.4, -22.32 \pm j46.68$
L=0.016H, C=0.001F		$-7.3 \pm j175.3, -19.6 \pm j44.12$
L=0.008H,C=0.005F		$-5.18 \pm j103.1, -21.17 \pm j47.15$

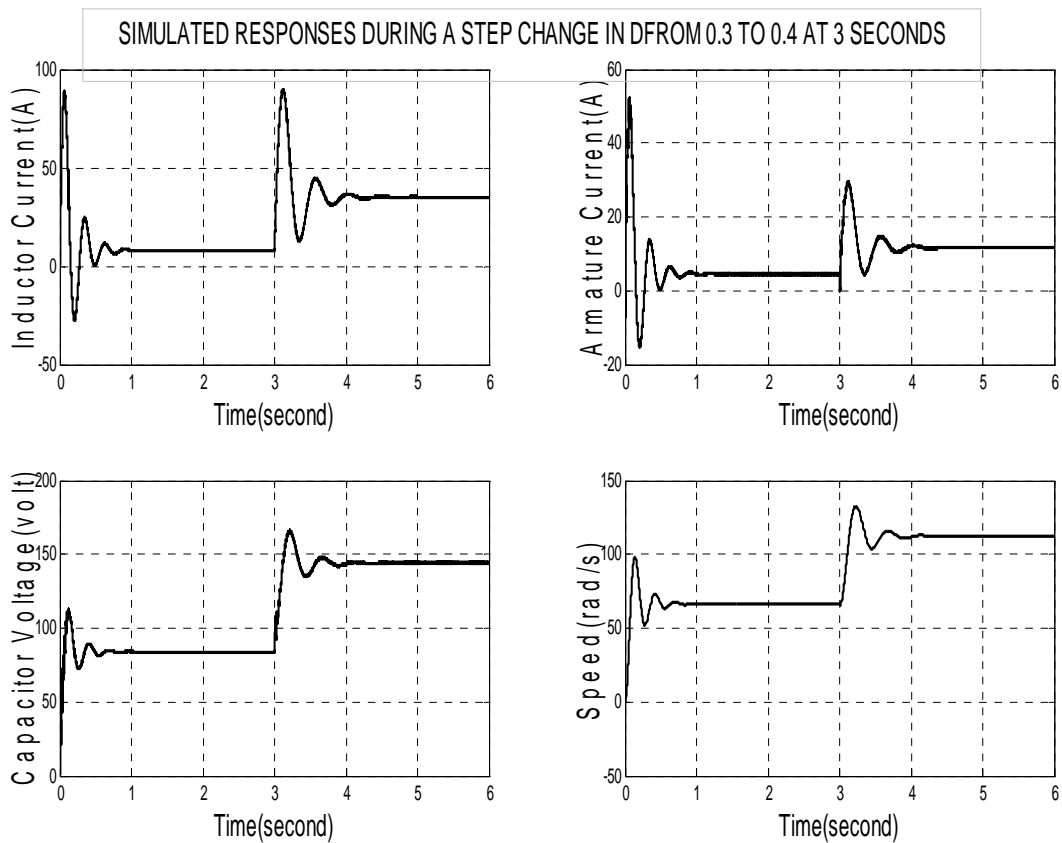


Fig. 9(a, b, c, d). Simulated response of Z-source inductor current, armature current, capacitor voltage and speed during a step change in D from 0.3 to 0.4 respectively

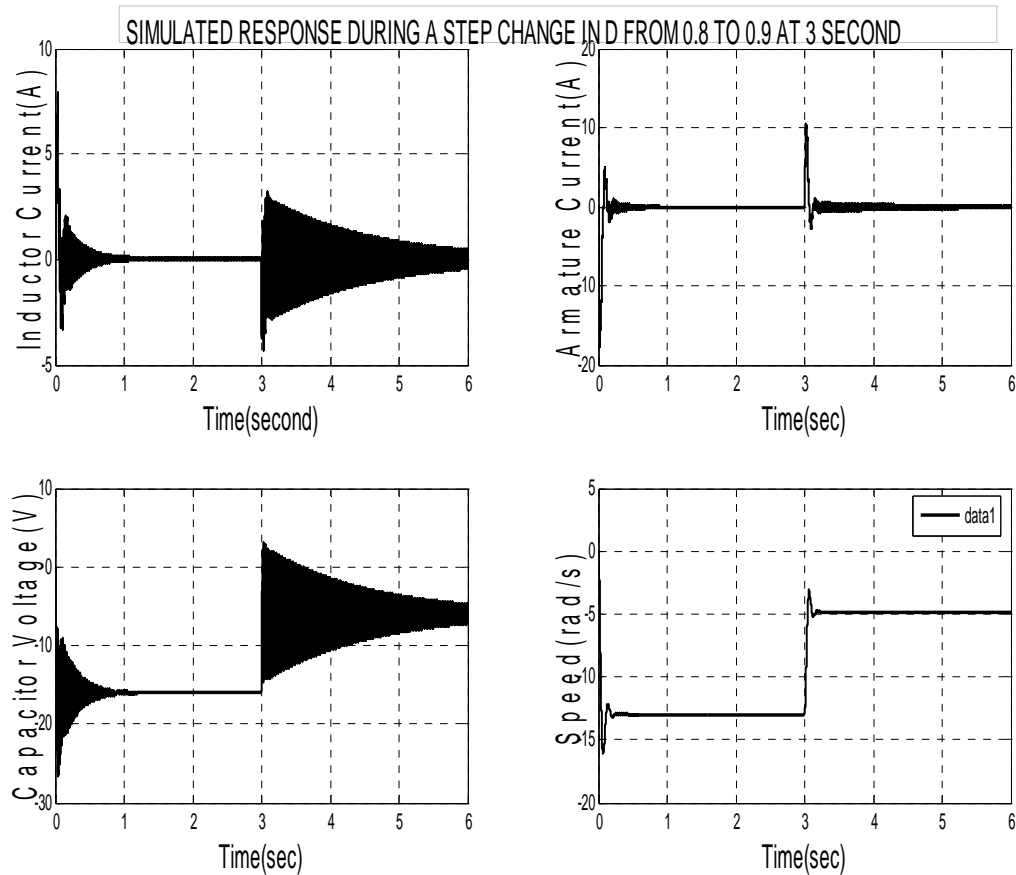


Fig. 10(a, b, c, d). Simulated response of Z-source inductor current, armature current, capacitor voltage and speed during a step change in D from 0.8 to 0.9 respectively

VII. CONTROL AND COMPENSATOR DESIGN

In order to keep the flow rate constant for different head, the speed control of DC motor with centrifugal pump is required. The actual speed of the motor is compared with the command speed estimated from the head and the error is processed through a compensator. The output of the compensator is the inductor current command. In the current mode control method, the inner loop, where the direct measurement of inductor current is compared with the reference inductor current. The output is fed to hysteresis band modulator and the pulses are generated for the switches of Z-source converter. Based on small signal model of z-source chopper with DC motor load and centrifugal pump set the closed loop speed control is shown in Fig.11.the compensator is designed based upon frequency responses.

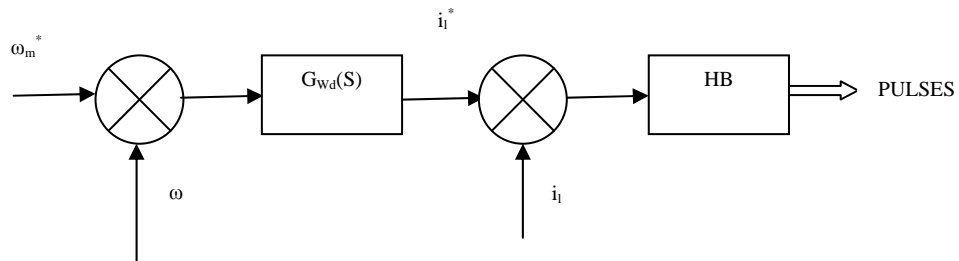


Fig.11 Block diagram of closed loop speed control of DC motor with centrifugal pump

The compensator bode plot and the plant bode plot is illustrated in Fig.12 (a, b). Again the root locus and compensated bode plot for the control-to-speed transfer function is shown in Fig. 13. The compensator for speed loop used for speed control of dc motor drive is expressed as follows:

$$G_{wd}(S) = 1.72 \times 10^{-10} \frac{(1+420S)}{s} \tag{28}$$

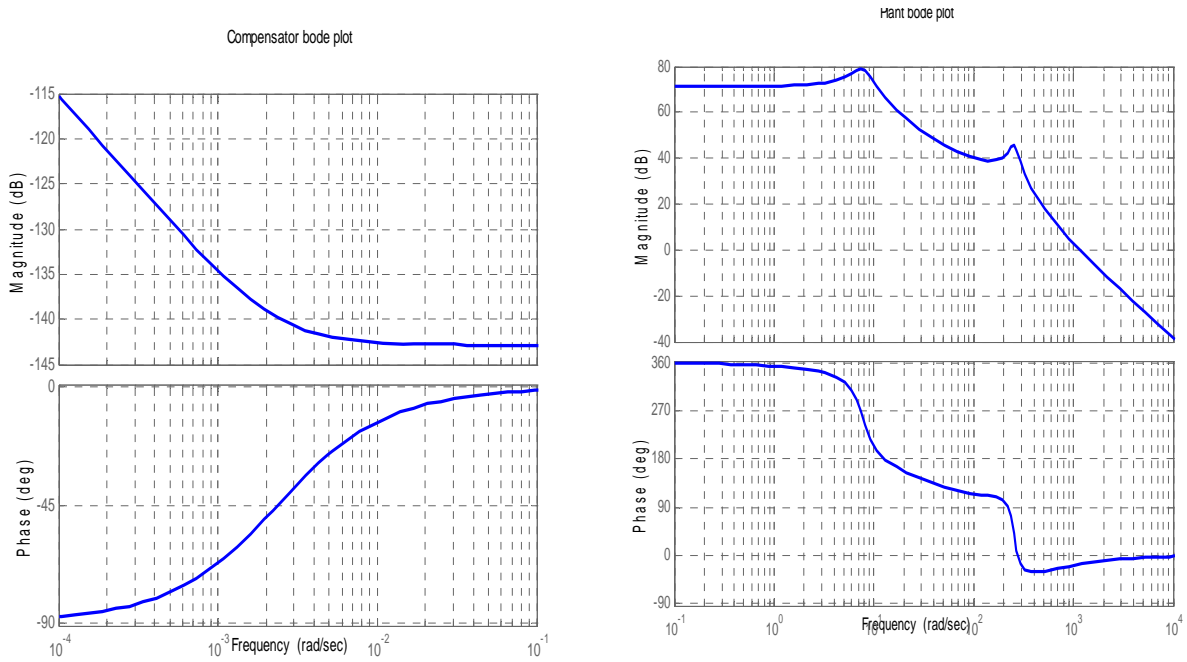


Fig.12 (a, b) compensator bode plot and plant bode plot.

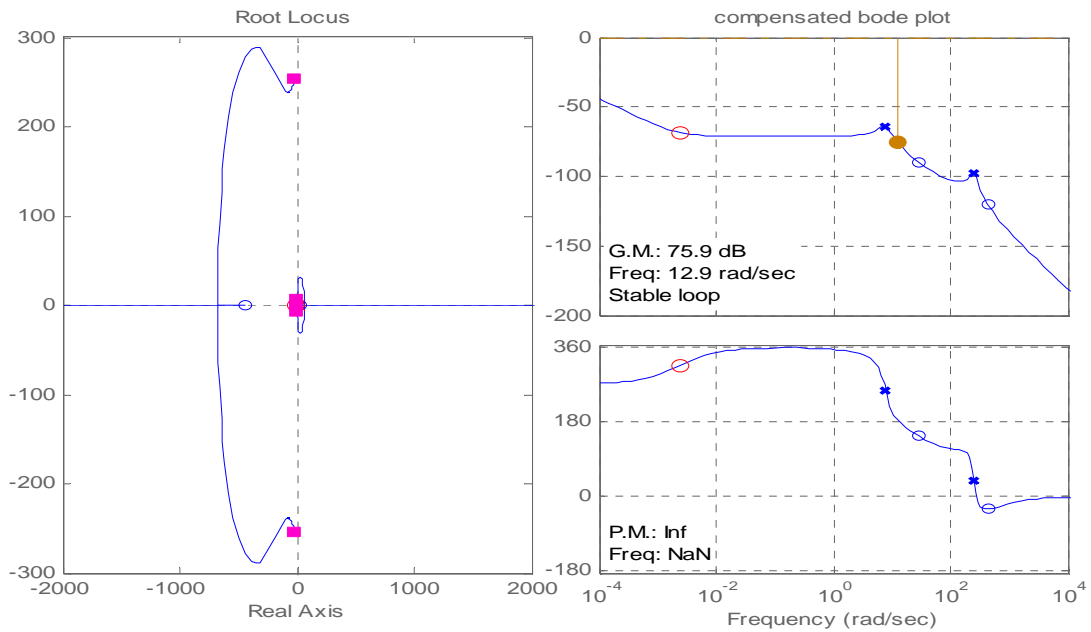


Fig.13 Root locus and Bode plot of compensated control to speed.

VIII. SIMULATION RESULTS

The compensator for speed loop is designed using (31). Step responses of 70 rad/s for 5 seconds and at 5 seconds step response command increased to 120 rad/s are used to observe the dynamic characteristics of speed, inductor current, armature current and capacitor voltage respectively. The three modes of operations are verified for the Z-source converter with centrifugal pump set. The inductor current, armature current and capacitor voltage and speed responses of change of step reference from 70rad/s to 120rad/s is shown in Fig. 14, Fig. 15, Fig. 16, Fig. 17 respectively. It has been observed that both of the speed responses reach the respective steady state value without exhibiting the oscillation. The settling time for high speed response is higher than the low speed step response command. Settling time for 70rad/s is 2.6 seconds and for 120rad/s is about 9 seconds.

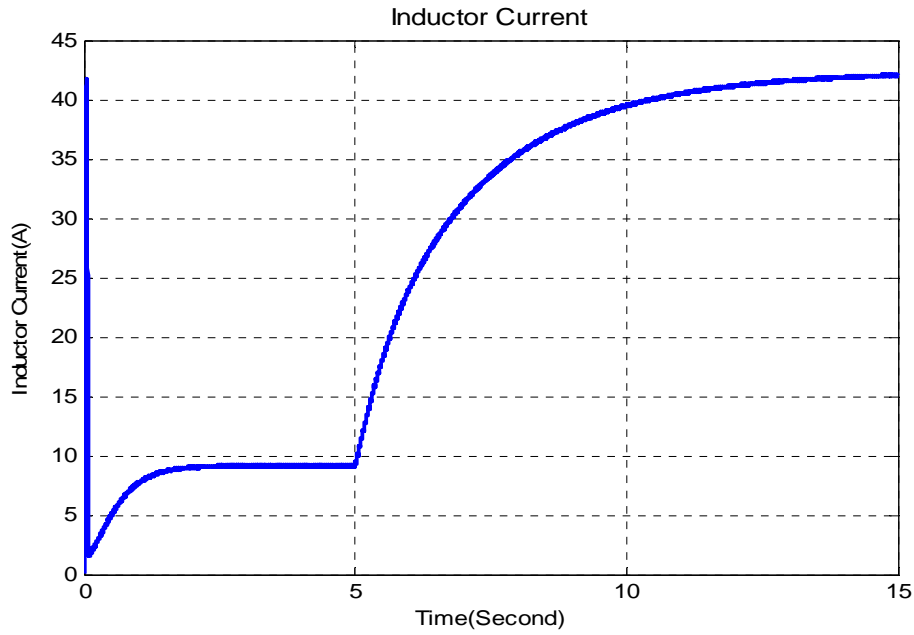


Fig.14 Inductor Current Response of closed loop Z-source chopper control of separately excited dc motor with centrifugal pump set for a change of step response from 70 rad/s to 120 rad/s.

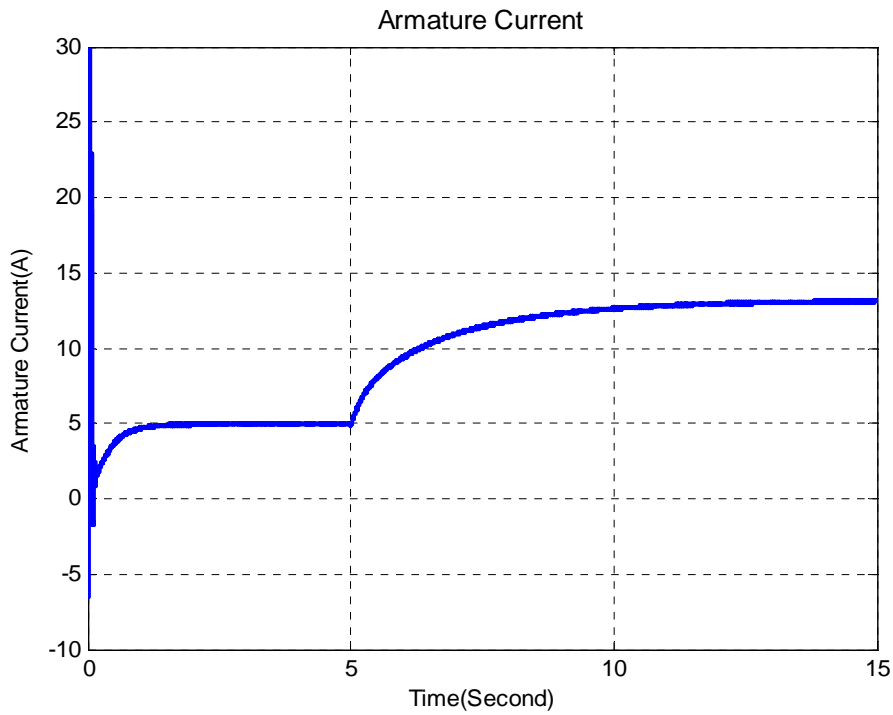


Fig.15 Armature Current Response of closed loop Z-source chopper control of separately excited dc motor with centrifugal pump set for a change of step response from 70 rad/s to 120 rad/s.

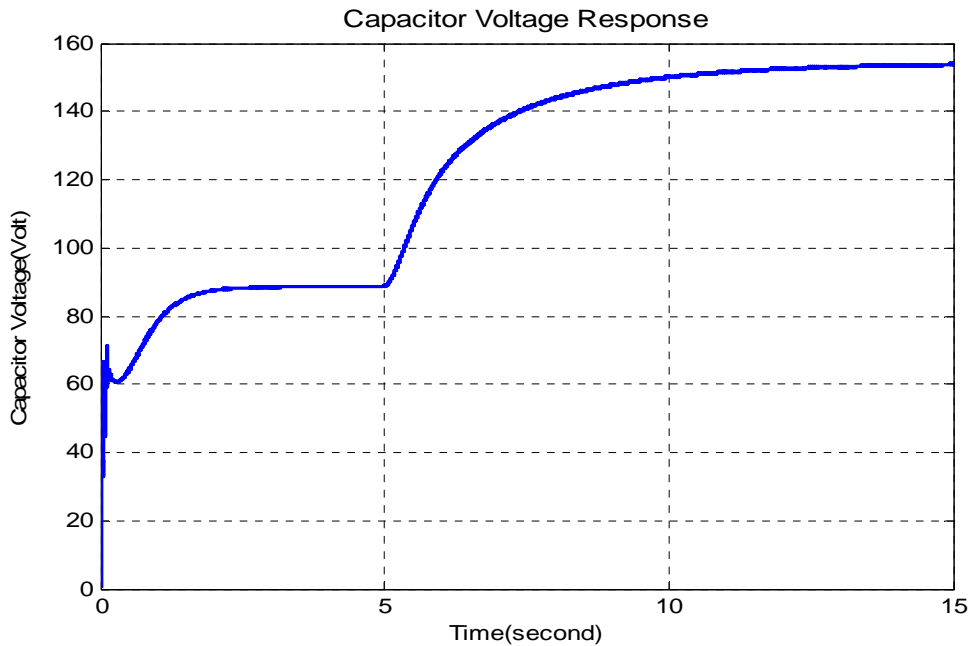


Fig.16 Capacitor Voltage Response of closed loop Z-source chopper control of separately excited dc motor with centrifugal pump set for a change of step response from 70 rad/s to 120 rad/s.

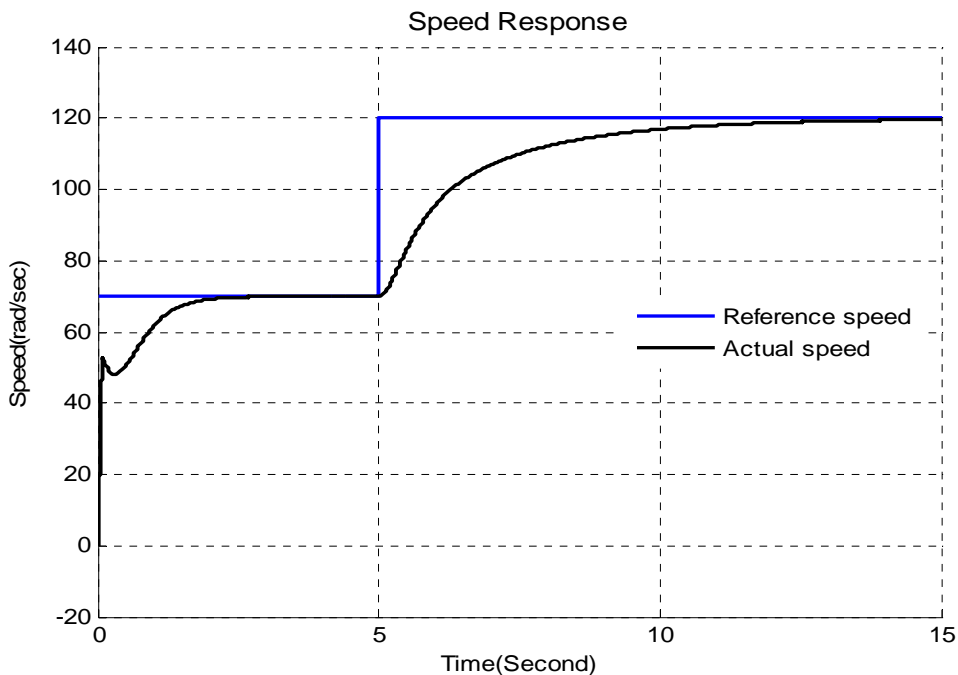


Fig.17 Speed Response of closed loop Z-source chopper control of separately excited dc motor with centrifugal pump set for a change of step response from 70 rad/s to 120 rad/s

IX. CONCLUSION

This paper presents the feedback Control and dynamic behaviour of Z-Source Converter Fed Separately Excited DC Motor and Centrifugal Pump Set. The study of transfer function of control-to-output has revealed that the existence of RHP zero which depend on passive parameters and control parameter causes dip in output responses due to sudden change of speed command. However, there is no dip in inductor current due to minimum-phase transient response caused by non existence of RHP zero of transfer function in boost mode with positive polarity. The inductor current feedback control is used to study the closed loop speed control of separately excited dc motor with centrifugal pump set, instead of armature current feedback. The compensators for the speed loop and the current loop are designed based on the frequency responses and as well as root locus

technique. The simulation responses of speed, inductor current, armature current and capacitor voltage for low speed and high speed are verified and presented.

X. APPENDIX

Machine rating and parameters: 5HP, 240V separately excited DC motor with $R_a=0.5\Omega$, $L_a=0.01H$, $K_b=1.23N\cdot m/Amp$, $R_f=240\Omega$, $J=0.05Kg\cdot m^2$, $B=0.02N\cdot m\cdot s/rad$ and No load speed= $193.8rad/s$.

REFERENCES

- [1] F.Z.Peng, "Z-source inverter," IEEE Transactions in Industry applications, vol.39, pp.504-510, Mar./Apr.2003.
- [2] R.Krishnan, Electric motor drives modeling, analysis and control, Pearson education pvt.ltd. 2003.
- [3] L.Umanand, Power electronic essentials and applications, vol. I. New York: Wiley publishers, 2009.
- [4] F.Z.Peng, X.M.Yuan, X.P.Fang, and Z.M.Quin, "Z-source inverter for adjustable speed drives," IEEE transactions in Power Electronics, vol. 1, pp.33-35, Jun.2003.
- [5] B.K.Nayak, Saswati Swapna Dash, "Battery Operated Closed Loop Speed Control of DC Separately Excited Motor by Boost-Buck Converter", IEEE International conference on power electronics (IICPE-2012), Dec., 2012.
- [6] B.K.Nayak, Saswati Swapna Dash, "Performance Analysis of Different Control Strategies in Z-source Inverter", ETASR – Engineering, Technology & Applied Science Research, vol. 3, pp.391-395. 2013,
- [7] Gokhan Sen and Malik Elbuluk, "Voltage and Current Programmed Modes in control of the Z-Source Converter," IEEE Transaction on Industry Applications, vol.46, pp.680-686, March/April.2010.
- [8] Poh.Chiang Loh, D.M.Vilathgamuwa, C.J.Gajanayake and C.W.Teo, "Transient Modelling and Analysis of Pulse-width modulated Z-Source Inverter," IEEE Transactions in Power Electronics, vol.22, pp.498-507, Mar. 2007.
- [9] B. Nayak and S. S. Dash, "Transient modeling of Z-source chopper used for adjustable speed control of DC motor drive," IEEE Fifth Power India Conference, pp. 1-6, Dec. 2012.
- [10] M.A.Elegendy, B.Zahawi, and D.J. Atkinson, "Comparison of directly connected and constant voltage controlled photovoltaic pumping systems," IEEE Transactions in sustainable energy, vol.1, pp.184-192, Oct. 2010.
- [11] R.Andoulssi, A.Draou, H.Jerbi, A.Alghonamy, B.Khiari, "Non linear control of a photo voltaic pumping system," Energy Procedia 42(2013), Elsevier, pp.328-336, 2013.
- [12] K.Smedley, and S.Cuk, "Switching flow graph nonlinear modelling technique," IEEE Transactions in Power Electronics, vol.9, pp.405-413, Jul.1994.
- [13] R.D.Middlebrook and S.Cuk, "A general unified approach to modelling switching converter power stages," in Proc.1976 IEEE PESC, pp.18-34, 1976.
- [14] P.Krein, Elements of Power Electronics, New York: Oxford University Press, 1998.
- [15] C.J.Gajanayake, D.Mahinda and Poh.Chiang Loh, "Small-Signal and Signal-Flow-Graph Modelling of Switched Z-source Impedance Network," IEEE Power Electronics Letter, vol.3, Sept.2005.
- [16] Kelvin R. Aaron, Noreen L. Foster, Danielle P. Hazel and A. M. Hasanul Basher, "Closed-loop position control system using lab VIEW," in Proc., Southeast conf, pp.283-286, 2002.
- [17] J.T.Humphries and L.P.Sheets, Industrial electronics, Bretor publishers, 1983.
- [18] G.F.Franklin, J.D.Powel and A.Emami-Naeini, Feedback Control of Dynamic Systems, 3rd ed. Reading, MA: Addison-Wesley, 1994.